Available online at www.sciencedirect.com
ScienceDirect
Trans. Nonferrous Met. Soc. China 25(2015) 2438−2445
Transactions of Nonferrous Metals Society of China
www.tnmsc.cn

Directional growth behavior of α(Al) dendrites during concentration-gradient-controlled solidification process in static magnetic field

Lei LI[1], Bo XU[2], Wei-ping TONG[1], Li-zi HE[1], Chun-yan BAN[1], Hui ZHANG[1], Yu-bo ZUO[1], Qing-feng ZHU[1], Jian-zhong CUI[1]

1. Key Laboratory of Electromagnetic Processing of Materials, Ministry of Education, Northeastern University, Shenyang 110819, China;
2. School of Metallurgy and Energy, Hebei United University, Tangshan 063009, China

Received 19 September 2014; accepted 20 January 2015

Abstract: The large and small sized Cu (solid)/Al (liquid) couples were prepared to investigate the directional growth behavior of primary α(Al) phase during a concentration-gradient-controlled solidification process under various static magnetic fields (SMFs). The results show that in the large couples, the α(Al) dendrites reveal a directional growth character whether without or with the SMF. However, the 12 T magnetic field induces regular growth, consistent deflection and the decrease of secondary arm spacing of the dendrites. In the small couples, the α(Al) dendrites still reveal a directional growth character to some extent with a SMF of ≤5 T. However, an 8.8 T SMF destroys the directional growth and induces severe random deflections of the dendrites. When the SMF increases to 12 T, the α(Al) dendrites become quite regular despite of the consistent deflection. The directional growth arises from the continuous long-range concentration gradient field built in the melt. The morphological modification is mainly related to the suppression of natural convections and the induction of thermoelectric magnetic convection by the SMF.

Key words: α(Al) dendrite; diffusion couple; concentration gradient field; static magnetic field; directional growth; thermoelectric magnetic convection

1 Introduction

Directional solidification is a technique in which the crystal growth occurs in a given direction that is opposite to the direction of heat flow. Due to its uniqueness in producing an anisotropic and oriented structure, this technique has been employed in electromagnetic processing of materials, and some quite interesting phenomena have been found [1−5]. In these experiments, a specially designed installation (such as Bridgman Stock-barge-type furnace [4,5]) was indispensable to establish a certain temperature gradient to ensure soundness. A careful observation on the binary alloy phase diagrams may bring about a new idea to realize directional growth of crystals with conventional solidification equipment (the heat flow is non-directional and the grains are usually equiaxed [6,7]). It is known that binary alloys with different compositions usually correspond to different liquidus temperatures. Given that a continuous long-range concentration gradient field (LRCGF) could be built in the melt, a temporal and spatial difference in the crystallization of the local melt would probably lead to directional growth of crystals and multiple microstructures during the synchronous cooling process. Such a field can be realized through preparing a solid/liquid diffusion couple. Additionally, considering that abundant microstructure changes can be induced by the electromagnetic field [8,9], some interesting phenomena may be obtained if such couples are treated under a static magnetic field (SMF).

So far, experiments based on such a conception have not been carried out. WANG et al [10], TANAKA et al [11] and LI et al [12] have ever annealed solid (Cu)/liquid (Al) diffusion couples, where some compound layers were found at the Cu−Al interface. But no directional crystal growth character was reported in their work, which was probably attributed to the small

Foundation item: Projects (51201029, 51071042, 51374067) supported by the National Natural Science Foundation of China; Projects (N130409002, N130209001) supported by the Research Funds for the Central Universities; Project (2012M520637) supported by the China Postdoctoral Science Foundation
Corresponding author: Lei LI; Tel: +86-24-83687734; E-mail: lilei@epm.neu.edu.cn
DOI: 10.1016/S1003-6326(15)63860-2

sizes of the couples where a LRCGF could not be formed. In the present work, the height of Al melt above the solid Cu in the couple was raised, and some quite original phenomena concerning directional crystal growth under SMF were carefully investigated.

2 Experimental

To verify the feasibility of the experiment, two types of couples with different sizes were designed. Firstly, two large Cu/Al diffusion couples were prepared, and each was produced as follows: a Cu disk (d15 mm × 5 mm; purity: 99.9% (mass fraction)) and an Al cylinder (d15 mm × 40 mm; purity: 99.99% (mass fraction)) were machined, polished and cleaned; the Cu disk was then put into a tube of corundum crucible, and the Al cylinder was thus placed on the disk. Secondly, seven small Cu/Al diffusion couples (Cu disk: d4 mm × 2 mm; Al cylinder: d4 mm × 10 mm) were also prepared using the same method as above.

Figure 1 shows the scheme of the experimental apparatus and the magnetic field distribution. The equipment consists of a vacuum resistance furnace installed in the bore of the magnet and a superconducting magnet that can produce an axial SMF (along Z direction) B with a maximum value of 12 T at the position Z=0 (i.e., $B_{Z=0}$=12 T), where the magnetic field can be regarded as relatively uniform within ±20 mm (when $B_{Z=0}$=12 T, $B_{Z=\pm 20\ mm}$=11.8974 T). A R-type thermocouple is used to measure the furnace temperature (the temperature field in the furnace is relatively uniform within ±75 mm as the temperature change is smaller than ± 5 °C).

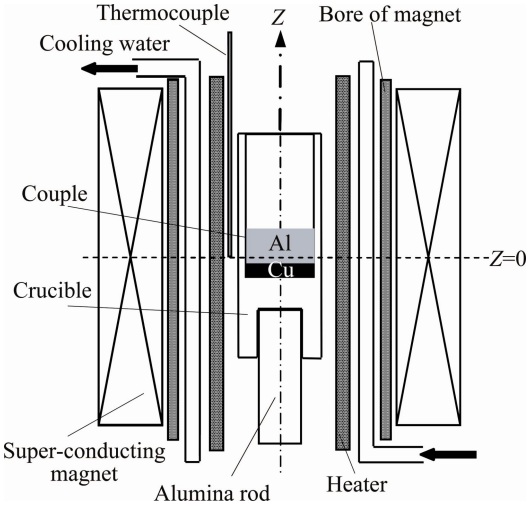

Fig. 1 Scheme of experimental apparatus and magnetic field distribution

In the present work, the couples were placed with their central sections at position Z=0. After the magnetic field reaching the set value, the couple was heated up to 680 °C under an argon atmosphere by an electric heater at a rate of 5 °C/min and held at 680 °C for 20 min to make the Al cylinder completely melted, and then cooled to room temperature at a rate of 5 °C/min. Finally, a solidified couple was obtained. The applied magnetic fields to different couples are given in Table 1.

Table 1 Applied magnetic fields to different couples

Couple	Magnetic fields/T
Large size	0 12
Small size	0 0.2 0.8 2 5 8.8 12

The specimens were cut lengthwise from the treated couples and then polished. The microstructures were observed with a Leica DMR microscope. The Cu compositions in the primary α(Al) matrix of the large sized couples were manually detected by an EPMA-1600/1610 electron probe microanalyer (EPMA) at intervals of 300 μm. The secondary dendrite arm spacing (SDAS) of the primary α(Al) dendrites of the large sized couples was measured with a combination of two common methods [13]: line intercept and individual arm counting.

3 Results

3.1 Large sized couples

Before showing the experimental results, it would like to firstly clarify that this work mainly aims at the directional growth of the primary α(Al) phase. Nevertheless, to give a general view to the readers, the multiple microstructures in the large sized couples are wholly displayed.

Figures 2(a) and (b) show the microstructures from the Cu end to the upper Al side (in the central part of the specimen) of the large sized couples without and with the 12 T SMF. The microstructural analysis indicates that the Eu region (between the two dashed lines 2 and 3) corresponds to the eutectics, whereas the upper Ho (above the dashed line 3) and the lower He (between the two dashed lines 1 and 2) regions represent the hypoeutectic and hypereutectic microstructures, respectively. Moreover, the Df region below the dashed line 1 belongs to the Cu/Al diffusion layers. In Fig. 2(d), the magnified BSE image of the intermediate layers at the Cu/Al interface without the SMF was also given (it should be mentioned that the application of the SMF did not induce obvious morphological change of the layers). As can be seen, five diffusion layers are distinguished clearly by different contrasts. Based on the Al−Cu phase diagram [14] and EPMA analysis, the five layers from the Cu end to the Al side are confirmed as β (Cu_3Al), γ_1 (Cu_9Al_4), ξ_2 ($Cu_{12}Al_9$), η_2 (CuAl) and θ ($CuAl_2$), respectively.

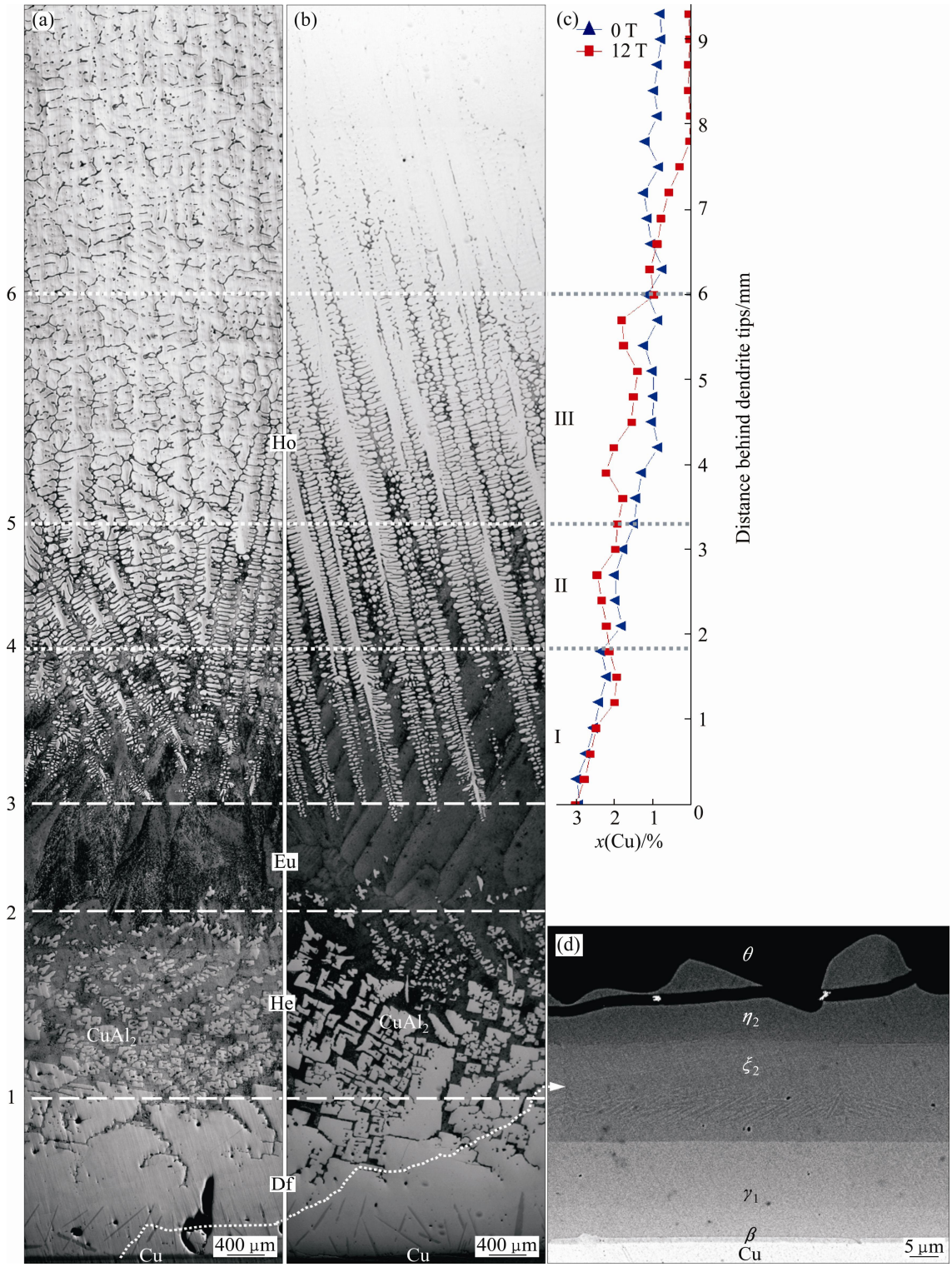

Fig. 2 Microstructures from Cu end to upper Al side of large sized couples without (a) and with (b) 12 T SMF, Cu composition (x(Cu)/%) in primary α(Al) matrix (c) as function of distance behind primary α(Al) dendrite tips, and magnified BSE image (d) of intermediate layers at Cu/Al interface without SMF

In the hypoeutectic microstructures without and with the SMF, the primary α(Al) phase reveals an obvious axial directional growth character that columnar grains grow approximately from the top down. However, a morphological discrepancy was also clearly demonstrated by the SMF. As shown in Fig. 2(a), without the SMF, the primary α(Al) dendrites grow irregularly and show some random deflections when they proceed to the final stage of growth. In contrast, when the SMF is applied, the primary α(Al) dendrites are less developed at

the beginning (above the dotted line 6 in Fig. 2(b)) and then more developed. The entire primary α(Al) phase reveals a regular array structure and a consistent deflection. These suggest that the application of SMF to the couple facilitates the regular growth of the α(Al) dendrites.

Furthermore, the SDAS of the primary α(Al) dendrites was also noticeably affected by the SMF. To facilitate the comparison of the SDAS, the α(Al) dendrites are partitioned into zones I, II and III based on the structure without the application of the SMF (in a single zone, the dendrites possess relatively uniform SDAS), as indicated by the dotted lines 4, 5 and 6 in Figs. 2(a) and (b) (considering the less developed dendrites with the SMF, the spacing measurement ends at line 6). Figure 3 shows the SDAS corresponding to the three zones without and with the SMF. Moving away from zone I into zone III, it can be found that in each case (without or with the SMF), the SDAS exhibits an increase, suggesting a coarsening process of the secondary arms. However, a side-by-side comparison shows that the SDAS is decreased by the SMF, but the SDAS in zone I are quite close with each other.

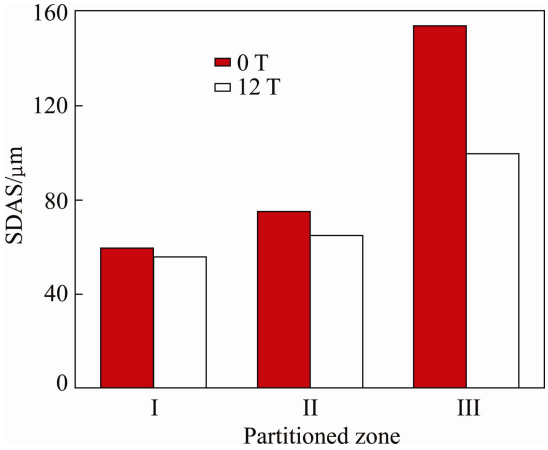

Fig. 3 SDAS of primary α(Al) dendrites in Figs. 2(a) and (b) corresponding to zones I, II and III without and with 12 T SMF

3.2 Small sized couples

To further identify the effects of the SMF on the directional growth of primary α(Al) dendrites, some small sized couples were also treated under various magnetic fields. Figures 4(a)−(g) show the top hypoeutectic microstructures of the small sized couples with SMFs of 0, 0.2, 0.8, 2, 5, 8.8 and 12 T, respectively. As can be observed, without the magnetic field, the α(Al) dendrites still reveal a directional growth character to some extent but show irregular deflections (Fig. 4(a)). With increasing the magnetic fields from 0.2 to 5 T

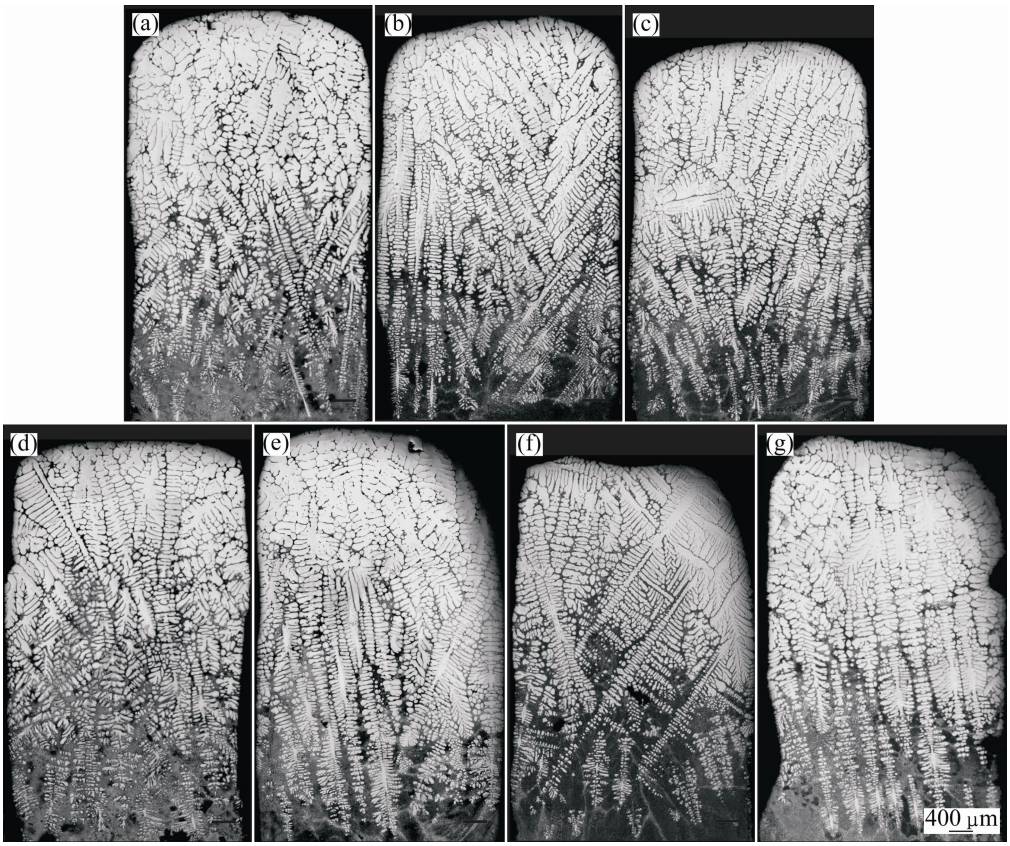

Fig. 4 Top hypoeutectic microstructures of small sized couples with SMFs of 0 T (a), 0.2 T (b), 0.8 T (c), 2 T (d), 5 T (e), 8.8 T (f) and 12 T (g), respectively

(Figs. 4(b)−(e)), both the directional growth character and irregularity do not change obviously. However, with a further increase of the SMF to 8.8 T (Fig. 4(f)), the α(Al) dendrites show quite weak directional growth character and severe random deflections. Interestingly, when the magnetic field further increases to 12 T, the α(Al) arrays become quite regular despite that they consistently deflect from the vertical axis for some degrees (similar to the case of the large sized couple with 12 T SMF (Fig. 2(b)).

4 Discussion

4.1 Large sized couple

As aforementioned, five intermediate diffusion layers at the Cu/Al interface were found. The formation of the diffusion layers has been explained in detail in Ref. [10], which is the result of a penetration process of liquid Al into solid Cu through reaction diffusion. Accompanying this process, the active Cu atoms also diffuse towards the upper Al melt, and the solute concentration decreases as the distance from the Cu end increases. Consequently, a LRCGF is probably formed.

According to the Al−Cu phase diagram shown in Fig. 5, a typical eutectic reaction (17% Cu, mole fraction) exists close to the Al end. When an appropriate LRCGF is built, the melt can contain hypoeutectic, eutectic and hypereutectic compositions simultaneously. If so, the local melt with a lower composition to the left of the eutectic point and that with a higher composition to the right of the eutectic point are firstly crystallized during the synchronous cooling process of the melt. For example, in the compositions *A*, *B* and *C* in Fig. 5, *A* obviously corresponds to the highest liquidus temperature. This means that the local melt with *A* composition will firstly crystallize, and then the melt with compositions *B* and *C* crystallize. This process

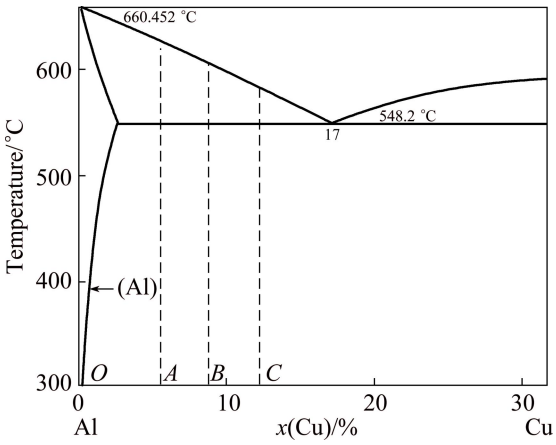

Fig. 5 Al−Cu phase diagram close to Al end (*A*, *B* and *C* correspond to three different compositions, showing different liquidus temperatures)

should be successive as the dendrite tips are always in a supercooled melt (resulting from the constitution change due to the formation of LRCGF), and will not cease until the composition ahead of the solidification front reaches eutectic point. These temporal and spatial differences in the local melt crystallization ultimately lead to directional crystal growth and multiple microstructures in the specimen. Of course, the radial heat transfer should also affect the growth of crystals. If the radial heat transfer becomes so dominated, the crystals may show a radial growth form rather than an axial one. However, the axial growth of primary α(Al) phase proves that the effect of the radial heat transfer can be neglected.

Despite this general analysis, the actual solute diffusion and crystal growth are affected by some other factors. During the diffusion process, natural convections (such as surface tension and thermocapillary convections) exist in the melt. In such a case, the mass transport is dominated by convections as the convective velocity is much greater than the diffusion velocity [15,16]. In other words, these convections enhance the mass transport. However, as these convections are usually irregular and unordered, the LRCGF may be disturbed and even become discontinuous and random. Furthermore, in the subsequent growth process, the solidifying of α(Al) dendrites will induce volume shrinkage and thus a fluid flow exists at the solid/liquid interface. This fluid flow plus the natural convections will cause thermal perturbation of the interface and induce irregular solute redistribution in the interdendritic regions (this redistribution should become more remarkable in the final stage of growth due to the increased composition). In other work [17], it has been found that convections can lead to a crystal growth deflection due to the concentration field change around a growing dendrite tip. All of these aspects result in the formation of randomly deflected columnar α(Al) crystals with irregular morphology (Fig. 2(a)). However, the application of a strong SMF (12 T in this work) can suppress these convections [18,19]. MIYAKE et al [20] showed that the obtained Sn−In diffusion coefficient data under high magnetic fields was the same order of magnitude as that measured under purely diffusive conditions in outer space (there was almost no any convection). Therefore, it is believed that the 12 T SMF in the present work should be also strong enough to suppress all the convections, and provides a stable environment to form a relatively continuous and regular LRCGF and a less disturbed thermal field, and thereby ensures the growth of regular α(Al) arrays (Fig. 2(b)).

The SDAS of the primary α(Al) dendrites is related to the effect of the SMF on the solute distribution. Due to the suppression of convections, the solute redistribution is dominated by diffusion. In other words, the SMF

attenuates the diffusion of Cu into the Al melt. Figure 2(c) shows the Cu composition (x(Cu)/%) in the primary α(Al) matrix as a function of the distance behind the dendrite tips without and with the SMF. Neglecting the rejected solutes to the solidifying interface and grain boundaries, it qualitatively reflects the tendency of the solute distribution in the original melt. It can be seen that the curve of 0 T shows a decrease first (<3.9 mm) and then tends to be moderate (>3.9 mm), whereas the curve of 12 T exhibits a slight decrease first (<6 mm) but then a sharp decrease (>6 mm). This solute distribution proves that the SMF tends to retard the diffusion of Cu atoms to the deep melt. The sharp decrease of Cu composition (x(Cu)→0) with the SMF may just explain that the primary α(Al) dendrites are less developed at the beginning (Fig. 2(b)) for no sufficient solute and thus constitutional supercooling induces fully developed secondary arms.

In Al−Cu alloy, it has been investigated by researchers that the SDAS decreased with increasing the solute concentration up to the eutectic composition [21]. Usually, the SDAS (λ_2) shows a strong dependence on the local solidification time (t_f) according to a power law [22]:

$$\lambda_2 = At_f^n \quad (1)$$

where A is a constant for the alloy system and n has a suggested value of 1/3 [23]. t_f can be approximated as $\Delta T_f/(GR)$, where ΔT_f is the equilibrium temperature range of solidification, G is the temperature gradient and R is the growth velocity. If G and R are simply regarded to be constant, it is natural that λ_2 decreases with increasing the composition. In the present work, when the partitioned zones in Figs. 2(a) and (b) are correlated with the x(Cu) distribution in Fig. 2(c), it can be found that the variation of the SDAS coincides with the analysis that from zone I to zone III (Fig. 3), a decreased x(Cu) corresponds to an increased SDAS in each case. However, it should also be noticed that even in an alloy with a fixed composition, the final SDAS in a fully solidified structure is usually much coarser than that forms initially [24]. This actually involves a coarsening process, which arises from that some of the initially formed arms remelt while others continue to grow. This should also contribute to the increase of λ_2 from zone I to zone III (zone III crystallizes firstly and has more time to coarsen). In Fig. 2(c), it can also be found that the x(Cu) with the SMF is higher than that without the SMF in zones II and III. As aforementioned, this results from the attenuation effect of the SMF on the diffusion of Cu atoms. This x(Cu) difference should be principally responsible for the decrease of λ_2 when the SMF is applied (In zone I, the x(Cu) and thus the SDASs with and without the SMF are approximately equal to each other).

4.2 Small sized couple

As aforementioned, in the small sized couples, the primary α(Al) dendrites also show directional growth character but possess various morphologies with different magnetic fields. The directional growth originates from the LRCGF but is affected by natural convections, which has been analyzed in detail above. However, the variation of the morphologies may also involve another type of convection−thermoelectric magnetic convection (TEMC). Despite that the measured temperature field in the furnace is relatively uniform on a large scale (the temperature change smaller than ±5 °C within ±75 mm), temperature gradients at the local solid/liquid interface should still exist. Due to the Seebeck effect, thermoelectric current in liquid metal will be produced [2,25]. The interaction of the thermoelectric current with the applied magnetic field will create thermoelectric force to drive the interdendritic melt to flow. This flow is the so-called TEMC. Similar to other convections, TEMC can promote mass and heat transport and affect crystal growth. However, the TEMC also tends to be suppressed by the SMF. Therefore, there should be a maximum flow velocity when the TEMC is balanced with the suppression. During a directional solidification process, LI et al [26] showed that when the magnetic field B increases, the flow velocity u increases for weak magnetic field values (u~$B^{1/2}$) while it decreases for large magnetic field amplitude (u~B^{-1}). The maximum magnetic field B_{max} corresponding to the maximum velocity is expressed as follows:

$$B_{max} = \left(\frac{\rho SG}{\lambda\sigma}\right)^{1/3} \quad (2)$$

where ρ is the density of the melt, S is the thermoelectric power, G is the temperature gradient, λ is a typical length scale, and σ is the electrical conductivity of the melt. In this work, some parameters, such as S and G, cannot be evaluated precisely, therefore it is not easy to obtain the real B_{max}. However, such an expression theoretically proves the existence of a maximum magnetic field which can induce a maximum flow velocity. Such a maximum flow velocity corresponds to the strongest TEMC. Similar to the natural convections, this TEMC should be also irregular and unordered, then disturbs the LRCGF and thus the directional growth of the α(Al) dendrites. According to the microstructures in Fig. 4, it may be induced that a value approximate to 8.8 T (Fig. 3(f)) may correspond to the strongest TEMC. Just due to this TEMC, the α(Al) dendrites show quite weak directional growth character and severe random deflections (Fig. 3(f)). Interestingly, in the Cu/Al couples treated by different SMFs, WANG et al [10] found that the curve of the measured thickness of diffusion layers exhibits a monotonic decrease with a superposed peak centered on

a field of 8.8 T, i.e., all the layers composed of different phases have the maximum thickness under a magnetic field of 8.8 T. They also attributed this to the strongest TEMC induced by a field of 8.8 T. Such phenomena and explanation agree well with what shown in this work. When the magnetic field further increases to 12 T, all kinds of convections, including the TEMC, are completely suppressed. Without the disturbance of convections, the α(Al) dendrites reveal regular arrays (Fig. 3(g)).

In addition, it has been shown that the α(Al) dendrites in both the large and small sized couples reveal a consistent deflection from the vertical direction. As a matter of fact, an analogous deflection phenomenon has also been found in the directional solidification process of hypoeutectic Al−Cu alloy under a SMF [27]. In the discussion of this phenomenon, the authors denied the possibility that the deflection of the α(Al) dendrites was induced by magnetization force as the magnetic crystalline anisotropy of the α(Al) dendrite was quite weak. Instead, they attributed it to the thermoelectric magnetic force (TEMF). The basic idea is that thermoelectric currents can be induced not only in the liquid but also in the solid owning to the Seebeck effect. Thus, TEMF will be produced to act on the dendrites. The magnitude order of the TEMF is expressed as follows [27]:

$$\mathrm{TEMF}=\frac{\sigma_{\mathrm{L}}\sigma_{\mathrm{S}}f_{\mathrm{L}}}{\sigma_{\mathrm{L}}f_{\mathrm{L}}+\sigma_{\mathrm{S}}f_{\mathrm{S}}}\left(S_{\mathrm{S}}-S_{\mathrm{L}}\right)GB \tag{3}$$

where σ_{L} and σ_{S} are the electrical conductivities of the liquid and solid phases, respectively, f_{L} and f_{S} are the fractions of the liquid and solid, respectively, S_{L} and S_{S} are the thermoelectric powers of the liquid and solid phases, respectively, and G is the temperature gradient. According to the authors, the TEMF acting on the tip and bottom of the α(Al) dendrites leads to a shear stress to deflect the dendrite trunk. However, it can be found in Eq. (3) that, the temperature gradient G plays an important role in determining the magnitude of the TEMF. In Ref. [28], the temperature gradient for numerically calculated TEMF was 60 K/cm. With some other parameters, it was obtained that the value of TEMF was of the order of 10^5 N/m^3 under a 10 T magnetic field. In the present work, as aforementioned, temperature gradient at the local solid/liquid interface should exist. However, it is almost impossible to reach a value of 60 K/cm under the present solidification condition. Based on this, the deflection of the α(Al) dendrites cannot be simply attributed to the TEMF. Unfortunately, at present, it cannot give a logical explanation to such a confusing phenomenon. Therefore, a further investigation is needed in the future.

Finally, just due to the composition segregation, such couples resemble the so-called “functionally graded material”, which shows a variation in the composition and structure gradually over the volume, leading to corresponding changes in the properties of the material. Therefore, they may have potential application values.

5 Conclusions

1) In the large couples, the α(Al) dendrites reveal a directional growth character whether without or with the SMF. However, the 12 T SMF leads to a consistent deflection of the regular arrays and decreases the SDAS.

2) In the small couples, the α(Al) dendrites still show a directional growth character to some extent when the SMF is ≤5 T. With an 8.8 T SMF, the α(Al) dendrites reveal quite weak directional growth character and severe random deflections. When the SMF increases to 12 T, the α(Al) dendrites exhibit regular arrays but deflect from the vertical direction for some degrees.

3) The directional growth of α(Al) dendrites results from LRCGF in the Al melt. The SMF-induced results originate from the suppression of natural convections and the induction of thermoelectric magnetic convection and thus the modification of the thermal and solute fields in the melt.

4) A question is left to be solved in the future, i.e., what results in the consistent deflection of the α(Al) dendrites.

References

[1] VERHOEVEN J D, PEARSON D D. The effect of a magnetic field upon directional solidification of Sn−Cd and Sn−Pb alloys [J]. Journal of Materials Science, 1973, 8(10): 1409−1412.

[2] TEWARI S N, SHAH R, SONG H. Effect of magnetic field on the microstructure and macrosegregation in directionally solidified Pb−Sn alloys [J]. Metallurgical and Materials Transactions A, 1994, 25(7): 1535−1544.

[3] ALBOUSSIERE T, NEUBRAND A C, GARANDET J P, MOREAU R. Magnetic field and segregation during Bridgman growth [J]. Magnetohydrodynamics, 1995, 31(3): 228−235.

[4] LI X, REN Z M, CAO G H, GAGMOUD A, FAUTRELLE Y. Influence of an axial uniform magnetic field on the solid/liquid interface curvature and macrosegregation in directionally solidified the Al−0.85 wt.% Cu alloy [J]. Materials Letters, 2011, 65(21−22): 3340−3343.

[5] LI X, REN Z M, FAUTRELLE Y, GAGMOUD A, ZHANG Y D, ESLING C. Degeneration of columnar dendrites during directional solidification under a high magnetic field [J]. Scripta Materialia, 2009, 60(6): 443−446.

[6] LI L, ZHANG Y D, ESLING C, JIANG H X, ZHAO Z H, ZUO Y B, CUI J Z. Influence of a high magnetic field on the precipitation behaviors of the primary Al_3Fe phase during the solidification of hypereutectic Al−3.31wt%Fe alloy [J]. Journal of Crystal Growth, 2012, 339(1): 61−69.

[7] LI L, ZHANG Y D, ESLING C, QIN K, ZHAO Z H, ZUO Y B, CUI J Z. A microstructural and crystallographic investigation on the precipitation behaviour of primary Al_3Zr phase under high magnetic

field [J]. Journal Applied Crystallography, 2013, 46(2): 421−429.
[8] CHEN Guo-qing, REN Xiao, ZHOU Wen-long, ZHANG Jun-shan. Atomic interdiffusion in Ni−Cu system under high magnetic field [J]. Transactions of Nonferrous Metals Society of China, 2013, 23(8): 2460−2464.
[9] LI Chuan-jun, REN Zhong-ming, REN Wei-li, WU Yu-qin. Nucleation and growth behaviors of primary phase in hypoeutectic Al−Cu alloy in high magnetic field [J]. Transactions of Nonferrous Metals Society of China, 2012, 22(S1): s1−s6.
[10] WANG Qiang, LI Dong-gang, WANG Kai, WANG Zhong-ying, HE Ji-cheng. Effects of high uniform magnetic fields on diffusion behavior at the Cu/Al solid/liquid interface [J]. Scripta Materialia, 2007, 56(6): 485−488.
[11] TANAKA Y, KAJIHARAB M, WATANABE Y. Growth behavior of compound layers during reactive diffusion between solid Cu and liquid Al [J]. Materials Science and Engineering A, 2007, 445−446: 355−363.
[12] LI X, LU Z Y, FAUTRELLE Y, SAADI B, REN Z M, DEBRAY F. Influence of strong magnetic field on interdiffusion behavior between Al and Cu [J]. Materials Letters, 2013, 96: 104−108.
[13] SPEAR R E, GARDNER G R. Dendrite cell size [J]. Transactions of the American Foundrymen's Society, 1963, 71: 209−215.
[14] RIANI P, ARRIGHI L, MARAZZA R, MAZZONE D, ZANICCHI G, FERRO R. Ternary rare-earth aluminum systems with copper: A review and a contribution to their assessment [J]. Journal of Phase Equilibria and Diffusion, 2004, 25(1): 22−52.
[15] INATOMI Y. Buoyancy convection in cylindrical conducting melt with low Grashof number under uniform static magnetic field [J]. International Journal of Heat and Mass Transfer, 2006, 49(25−26): 4821−4830.
[16] KASSEMI M, BARSI S, ALEXANDER J I D, BANISH M. Contamination of microgravity liquid diffusivity measurements by void-generated thermocapillary convection [J]. Journal of Crystal Growth, 2005, 276(3−4): 621−634.
[17] FLEMINGS M C, ADAMS C M, HUCKE E E, TALOR H F. Metal solidification in a flowing stream [J]. Transactions of the American Foundrymen's Society, 1956, 64: 636−639.
[18] CARRUTHERS J R. Preparation and properties of solid state materials [M]. New York: Marcel Dekker, 1977.
[19] MATTHIESEN D H, WARGO M J, MOTAKEF S, CARLSON D J, NAKOS J S, WITT A F. Dopant segregation during vertical Bridgman-Stockbarger growth with melt stabilization by strong axial magnetic fields [J]. Journal of Crystal Growth, 1987, 85(3): 557−560.
[20] MIYAKE T, INATOMI Y, KURIBAYASHI K. Measurement of diffusion coefficient in liquid metal under static magnetic field [J]. Japanese Journal of Applied Physics, 2002, 41(7A): L811−L813.
[21] YOUNG K P, KIRKWOOD D H. Dendrite arm spacings of aluminum−copper alloys solidified under steady-state conditions [J]. Metallurgical and Materials Transactions A, 1975, 6(1): 197−205.
[22] TUNCA N, SMITH R W J. Variation of dendrite arm spacing in Al-rich Zn−Al off-eutectic alloys [J]. Journal of Materials Science, 1988, 23(1): 111−120.
[23] KURZ W, FISHER D J. Fundamentals of solidification [M]. Aedermannsdorf: Trans Tech Publications, 1984.
[24] FLEMINGS M C. Solidification processing [M]. New York: McGraw-Hill, 1974.
[25] BOETTINGER W J, BIANCANIELLO F, CORIELL S. Solute convection induced macrosegregation and the dendrite to composite transition in off-eutectic alloys [J]. Metallurgical and Materials Transactions A, 1981, 12A(2): 321−327.
[26] LI X, FAUTRELLE Y, REN Z M. Influence of thermoelectric effects on the solid–liquid interface shape and cellular morphology in the mushy zone during the directional solidification of Al−Cu alloys under a magnetic field [J]. Acta Materialia, 2007, 55(11): 3803−3813.
[27] LI X, LI Q Y, REN Z M, FAUTRELLE Y, LU X G, GAGNOUD A, ZHANG Y D, ESLING C, WANG H, DAI Y M, WANG Q L. Investigation on the formation mechanism of irregular dendrite during directional solidification of Al−Cu alloys under a high magnetic field [J]. Journal of Alloys and Compounds, 2013, 581: 769−775.
[28] LI X, GAGNOUD A, FAUTRELLE Y, REN Z M, CAO G H, MOREAU R, ZHANG Y D, ESLING C. Investigation of thermoelectric magnetic force in solid and its effect on morphological instability in directional solidification [J]. Journal of Crystal Growth, 2011, 324(1): 217−224.

静磁场下浓度梯度控制的凝固过程中 α(Al)枝晶定向生长行为

李 磊[1]，徐 博[2]，佟伟平[1]，何立子[1]，班春燕[1]，张 辉[1]，左玉波[1]，朱庆丰[1]，崔建忠[1]

1. 东北大学 材料电磁过程研究教育部重点实验室，沈阳 110819；
2. 河北联合大学 冶金与能源学院，唐山 063009

摘 要：制备大小两种 Cu(固态)/Al(液态)扩散偶，考察在不同静磁场下浓度梯度控制的凝固过程中初生 α(Al)相的定向生长行为。结果表明：在大扩散偶中，无论是否施加磁场，α(Al)枝晶均呈现定向生长特征，但 12 T 磁场导致枝晶的规则生长、一致偏转和二次枝晶臂减小；在小扩散偶中，当磁感应强度≤5 T 时，α(Al)枝晶仍呈一定的定向生长特征，当磁感应强度升至 8.8T 时，枝晶的定向生长被破坏并诱发严重的混乱偏转，而当磁感应强度升至 12 T 时，枝晶尽管仍呈一致偏转，但变得非常规则。枝晶的定向生长源于在熔体中建立的连续长程浓度梯度。枝晶的形貌改变则主要与静磁场对自然对流的抑制以及其诱发的热电磁对流有关。

关键词：α(Al)枝晶；扩散偶；浓度梯度；静磁场；定向生长；热电磁对流

(Edited by Mu-lan QIN)